Self-mixing laser diode vibrometer

Guido Giuliani, Simone Bozzi-Pietra and Silvano Donati

Dipartimento di Elettronica, Università di Pavia, Via Ferrata 1, I-27100 Pavia, Italy

E-mail: giuliani@ele.unipv.it

Abstract
The principle and the experimental realization of a new type of laser
vibrometer based on the self-mixing interference effect in a laser diode are
presented. The self-mixing configuration allows for a practical set-up that is
simpler by far than conventional laser vibrometer schemes. The vibrometer
relies on locking of the system to half the interferometric fringe, and on
active phase-nulling by wavelength modulation. This allows an extended
dynamic range to be achieved, whilst retaining a good sensitivity to
sub-wavelength vibrations. We have designed and built a prototype of the
vibrometer that can operate on nearly any kind of rough surface, covering
the 0.1 Hz–70 kHz frequency range of vibration. The noise floor is less than
100 pm Hz$^{-1/2}$, and the maximum measurable vibration amplitude is
180 μm peak to peak. The proposed method can find application in modal
analysis and noise and vibration measurements in industrial and scientific
environments.

Keywords: vibration, displacement, laser interferometer, diode laser,
self-mixing, non-contact measurement, non-destructive measurement, laser
Doppler velocimetry, PZT, speckle

(Some figures in this article are in colour only in the electronic version)

1. Introduction

Laser vibrometry is a well established technique that allows
remote and contactless measurement of the vibration of a solid
target. It relies on the coherence properties of a laser beam, and
on the high sensitivity of the coherent detection exploited in a
Michelson interferometer, which permits us to detect the very
small echo signal backscattered by a rough diffusing surface.
Laser vibrometry has been demonstrated and successfully used
in a variety of scientific and industrial applications, where high
sensitivity and low invasiveness are of importance, e.g. modal
analysis, vibration and noise testing, characterization of
loudspeakers and piezoceramic transducers [1–4].

The standard approach to optical measurement of small
vibrations is laser Doppler velocimetry (LDV), on which
a number of commercial products have been developed.
The operating principle is that of conventional Michelson
and Mach–Zehnder interferometers. The measuring arm
projects light from a He–Ne laser onto a vibrating target,
the backscattered light undergoes a Doppler frequency shift
proportional to the target velocity and it is then coherently
detected at the instrument side. Unlike displacement

measuring interferometers, the interferometric signal is usually
processed by extracting the Doppler beat frequency through
a frequency demodulator, so as to obtain an output signal
proportional to the instantaneous target velocity. To remove
the sign ambiguity of the cosine signal, two remedies are used:

(i) doubling of the interferometer by the dual-polarization
technique that gives two quadrature signals;
(ii) frequency shifting of the local oscillator light by means
of an acousto-optic modulator followed by heterodyne
detection.

Commercial instruments can measure velocities ranging from
a few μm s^{-1} to 1000 mm s^{-1} (although a single instrument
hardly reaches a 100 dB dynamic range), for vibration
frequencies from 0.01 Hz to a few MHz [1–4].

In this work we present a new type of laser vibrometer [5]
based on a compact laser diode (LD) that is extremely
simple and versatile. It relies on the self-mixing
interferometric configuration [6–11], and on active phase-
nulling accomplished through LD wavelength modulation. In
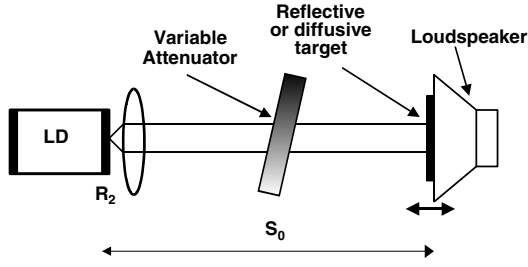the self-mixing interferometric configuration, light from the

Figure 1. Experimental set-up for self-mixing interferometric configuration. Light from an LD is focused or collimated by a lens onto a reflective or diffusive moving target. The variable attenuator is used to achieve the desired optical feedback strength.

LD is focused on the remote target, and a fraction of the backscattered light is allowed to re-enter the LD cavity. Here, it is coherently detected by the lasing field through a sort of mixing that generates a modulation onto the emitted power, so that the interferometric signal can be retrieved by the monitor photodiode included in the LD package. This well established interferometric configuration neither requires the reference arm nor large optical part count, hence the set-up is extremely simple and cheap [6–8]. The operating principle of the proposed vibrometer consists in locking of the interferometric phase to half a fringe by means of a feedback loop acting on LD wavelength. An additional phase-nulling technique allows us to greatly expand the dynamic range beyond the $\lambda/2$ fringe width. A prototype version of the instrument has been designed and built, which is capable of transducing vibrations of most rough diffusive surfaces with peak amplitude in the range between 0.1 nm and 90 μm, in a 0.1 Hz–70 kHz frequency range, and with good linearity.

2. Self-mixing interferometry

Self-mixing interferometry is nowadays a well established technique [6–11] capable of performing high accuracy measurement using a very simple arrangement. A typical experimental set-up is shown in figure 1. Light from a single-longitudinal-mode LD is projected onto a reflective or diffusive target, and a small fraction of the backreflected or backscattered light is allowed to re-enter the laser cavity, thus generating a modulation of both the amplitude and the frequency of the lasing field. It turns out that the power emitted by the LD is modulated by a waveform $F(\phi)$ which is a periodic function of the backinjected field phase $\phi = 2ks$, where $k = 2\pi/\lambda$ is the wavenumber and s is the distance from LD to target. At low levels of backreflection, $F(\phi)$ is the familiar $\cos(\phi)$ function, whereas at higher levels it becomes progressively distorted.

The power emitted by the LD can be written as

$$P(\phi) = P_0[1 + mF(\phi)] \tag{1}$$

where P_0 is the power emitted by the unperturbed LD and m is a modulation index. The modulation index m and the shape of the function $F(\phi)$ depend on the so-called *feedback parameter C* (after [12]):

$$C = \frac{s_0}{\sqrt{A_{opt}}} \frac{\varepsilon\sqrt{1+\alpha^2}}{L_{las}n_{las}} \frac{1 - R_2}{\sqrt{R_2}} \tag{2}$$

where $A_{opt} > 1$ is the total round-trip power attenuation in the external cavity, α (typically $\alpha = 3$) is the LD linewidth enhancement factor, $\varepsilon \leqslant 1$ (typically $\varepsilon = 0.5$) accounts for a mismatch between the reflected and the lasing modes, L_{las} is the laser cavity length, n_{las} is the cavity refractive index and R_2 is the LD output facet power reflectivity. The value of the C parameter depends on both the amount of optical feedback and on the target distance s_0. The C parameter is of great importance, because it discriminates between different feedback regimes. For $C \ll 1$ (very weak feedback) the modulation index m is directly proportional to $1/\sqrt{A}$, and the function $F(\phi)$ is a cosine, just like conventional interferometry. When C approaches unity the function $F(\phi)$ resembles a distorted cosine. For $C > 1$ (moderate feedback regime, which corresponds to an optical power attenuation of about 10^5, for a target distance $s_0 = 1$ m) the function $F(\phi)$ becomes sawtooth-like and exhibits hysteresis. In this regime the modulation coefficient m is around 10^{-3}, hence the available interferometric signal is large enough for an easy subsequent processing. Examples of an experimental interferometric waveform obtained in the different feedback regimes are reported in figure 2. Of particular interest are the waveforms of figures 2(d) and (e): they have a triangular shape and they exhibit sharp transitions every time the target is displaced by an amount $\lambda/2$. They also present a large hysteresis, which is responsible for the appearance of a two-level signal, with each level corresponding to one motion direction of the target. The properties of these waveforms have been exploited to demonstrate a displacement measuring interferometer, capable of reconstructing the motion of a target with $\lambda/2$ resolution without ambiguity from a single interferometric channel [8]. Interestingly, the self-mixing approach was previously investigated in He–Ne lasers by one of the authors as explained in [13], where the first complete interferometer/vibrometer based on the self-mixing effect was demonstrated.

Benefits of the self-mixing sensing scheme are the following:

(1) no optical interferometer external to the source is needed, resulting in a very simple, part-count-saving and compact set-up;
(2) no external photodetector is required, because the signal is provided by the monitor photodiode contained in the LD package;
(3) operation on targets with rough diffusive surface is possible, because the noise equivalent vibration of the scheme is very high, being a sort of coherent detection that easily attains the quantum detection regime (i.e., sub-nm noise equivalent vibration displacement);
(4) self-mixing interferometry is feasible with virtually all specimens of single-mode LDs;
(5) it is a very versatile approach, that has been deployed to measure displacement [6–8, 14], distance [15–17], velocity [18–20] and surface roughness [21].

3. Principle of self-mixing vibrometer

The self-mixing vibrometer is based on the idea of locking the interferometer phase to half a fringe, with the purpose of attaining a resolution and a noise equivalent vibration
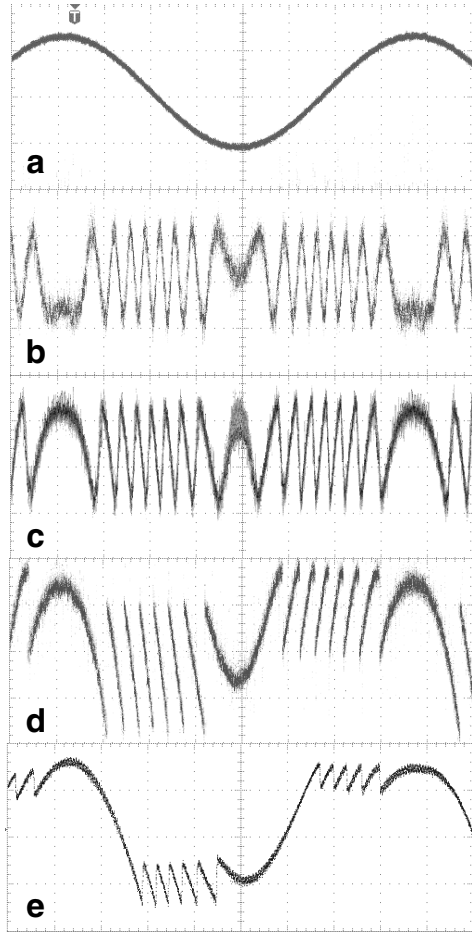
Figure 2. Examples of experimental interferometric waveforms obtained from the monitor photodiode using the self-mixing set-up shown in figure 1. (a) Loudspeaker drive signal at 657 Hz, calibrated so that the vertical scale corresponds to a displacement of 1.2 μm div^{-1}; timescale 200 μs div^{-1}. (b)–(e) Self-mixing signals obtained for increasing optical feedback strength. (b) Very weak feedback, vertical scale 2 mV div^{-1}; the interferometric waveform $F(\phi)$ is a cosine. (c) Weak feedback, vertical scale 10 mV div^{-1}; the interferometric waveform $F(\phi)$ is a distorted cosine. (d) Moderate feedback, vertical scale 20 mV div^{-1}; the interferometric waveform $F(\phi)$ is sawtooth-like and exhibits hysteresis. (e) Medium–strong feedback, vertical scale 50 mV div^{-1}; the interferometric waveform shows an increased hysteresis.

which are limited by shot noise and not by the quantization imposed by fringe counting. Besides this, an active phase-nulling technique allows us to extend the maximum measurable vibration well beyond the $\lambda/2$ fringe width.

In conventional LDVs, a vibration of arbitrary amplitude and waveform can in principle be retrieved without ambiguity and distortion, either owing to the availability of two interferometric quadrature channels, or to a heterodyne detection technique. This is also true for the He–Ne based self-mixing vibrometer demonstrated in a seminal paper [13], which makes use of both amplitude and frequency demodulation to extract the two quadrature signals. Conversely, when an LD is used in a self-mixing configuration, only one single interferometric channel is accessible, because the two-frequency regime required for heterodyning is not easily implemented with LDs, nor is a reference arm available.
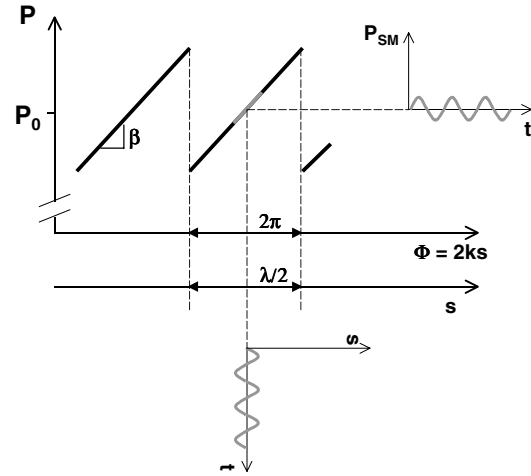

Figure 3. Principle of linear measurement of small target vibrations by locking the interferometer phase to half a fringe in the moderate feedback regime, where the interferometric signal can be approximated as having a triangular shape. The vertical axis represents the power emitted by the LD, where P_0 is the power emitted by the unperturbed LD; the horizontal axes represent interferometric phase and target displacement respectively.

Even with a single cosine interferometric signal, vibration measurements can be performed if the interferometer phase is locked to half a fringe. In this case, however, the vibration amplitude is limited to a value much smaller than $\pm\lambda/4$ if non-linearities are to be avoided. To this extent, the self-mixing approach operated in the moderate feedback regime offers a first advantage. In fact, due to the sawtooth-like triangular interferometric waveform (see figures 2(d) and (e)) the maximum vibration amplitude that can be linearly transduced is increased to at least $\lambda/4$. This is shown in figure 3, where the principle of locking to half a fringe is also illustrated. A viable method to lock the interferometer phase to half a fringe is to use an electronic feedback loop that counteracts on LD wavelength, so as to compensate for slow phase variations caused by environmental and thermal fluctuations. This sensing scheme has a remarkable noise equivalent vibration, which is solely limited by the shot noise of the photodetected current. Calculations show that for an LD emitting 10 mW power, and a vibrating diffusive target placed at 0.1 m distance, the noise equivalent vibration can be as low as a few pm Hz$^{-1/2}$ (see section 4.1).

Still within the concept of locking to half a fringe, another technique can be used to expand the dynamic range of the sensor, e.g. the maximum measurable vibration amplitude. We call this the 'active phase-nulling' technique, and its principle is that the feedback loop is also used to compensate for interferometric phase variations that are caused by the displacement of the target itself. In other words, the LD wavelength must be changed so as to keep a constant number of wavelengths in the physical path from LD to target; e.g., if the target moves away from the LD, then LD wavelength must be suitably increased. This is basically the approach used in common servo-sensor schemes, here applied to an optical interferometer.

Let the interferometer phase be $\phi = 2 \times (2\pi/\lambda)s$. If we now differentiate this expression with respect to s and λ,
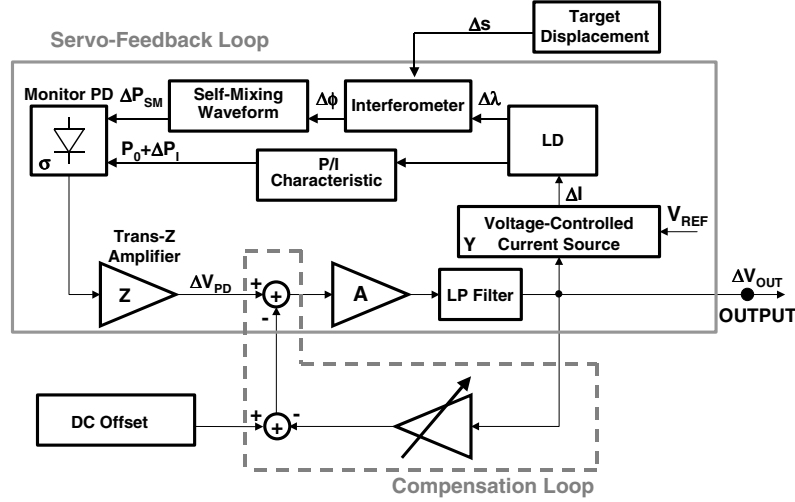
Figure 4. Block scheme for the self-mixing vibrometer accomplishing the phase-locking and phase-nulling techniques. Input and output variables for each block are shown, in accordance with equations (5)–(10) in the text.

we obtain

$$\Delta\phi = 2 \times 2\pi/\lambda_0 \Delta s - 2 \times 2\pi/\lambda_0^2 s_0 \Delta\lambda \qquad (3)$$

where s_0 is the distance from LD to target at rest, and λ_0 is the emitted wavelength at rest. The purpose of the feedback loop is to keep the interferometer phase constant, i.e. $\Delta\phi = 0$. This means that the phase change caused by the target displacement Δs is compensated by applying a wavelength variation $\Delta\lambda$ to the LD, so that, from (3),

$$\Delta\lambda = (\lambda_0/s_0)\Delta s. \qquad (4)$$

The wavelength variation of the LD can be attained by acting on the LD current, using an LD driver with external signal modulation capability. The electrical output signal of the vibrometer is then represented by the 'amplified error' signal, which is fed to the LD driver. Using this approach, the dynamic range of the sensor can be greatly expanded beyond the value $\lambda/4$, by an amount that approximately corresponds to the open-loop gain of the system (see section 4 for a more detailed analysis). To properly work in the above proposed scheme, the only requisite that the LD shall satisfy is to possess a continuous wavelength tunability over a modest span (i.e. a few tens of pm), and this condition is fulfilled by most single-longitudinal-mode Fabry–Perot LDs.

4. System design and performance

In this section the block scheme of the self-mixing vibrometer is presented, along with the adopted design criteria. The responsivity, noise, maximum measurable vibration and the precision of the instrument are analysed.

The block scheme of the self-mixing vibrometer is shown in figure 4. The blocks contained in the solid box constitute the servo-feedback loop, and the blocks contained in the dashed box make up the compensation path. The main block is the self-mixing interferometer operating in the moderate feedback regime, whose phase must be kept at a constant value, corresponding to half an interferometric fringe. The

target displacement Δs acts as a perturbation to the system, and it generates a variation $\Delta\phi$ of the interferometric phase. Numerically, we have

$$\Delta\phi = 2 \times 2\pi/\lambda \Delta s. \qquad (5)$$

The phase variation $\Delta\phi$ causes a proportional variation ΔP_{SM} in the power emitted by the LD through the self-mixing effect, given by

$$\Delta P_{SM} = \beta\Delta\phi \qquad (6)$$

where β (W rad^{-1}) is the slope coefficient of the triangular transfer characteristic of the interferometer (see figure 3). The power variation is detected by the monitor PD and converted into the voltage signal ΔV_{PD} by the transimpedance amplifier:

$$\Delta V_{PD} = \sigma Z \Delta P_{SM} \qquad (7)$$

where σ (A W^{-1}) is net photodiode responsivity (accounting for both PD quantum efficiency and LD-to-PD coupling efficiency), and Z (Ω) is the transresistance. This signal is then amplified by a factor A, low-pass filtered, and fed to the input of the voltage-controlled LD current source with admittance Y, thus generating a variation ΔI of the LD current:

$$\Delta I = AY\Delta V_{PD}. \qquad (8)$$

This, in turn, gives rise to a variation $\Delta\lambda$ of the LD wavelength, given by

$$\Delta\lambda = \chi\Delta I \qquad (9)$$

where $\chi \equiv d\lambda/dI$ (m A^{-1}) is the coefficient of wavelength drift versus injected current. The feedback loop ensures that the phase variation generated by the LD wavelength variation be exactly opposite (at least at first order) to that caused by target displacement. The amplified error signal ΔV_{OUT} fed to the current source is a perfect replica of the target displacement and it constitutes the instrument output. When condition (4) is fulfilled, it follows from (5)–(9) that the responsivity of the instrument is given by

$$\Re \equiv \Delta V_{OUT}/\Delta s = \lambda_0/(s_0\chi Y). \qquad (10)$$

The responsivity is inversely proportional to the target distance at rest s_0, as confirmed by experimental results reported in figure 7. The above dependence may appear as a drawback, since s_0 is in principle not well known. Actually, this is not a major cause of uncertainty because, as will be explained in section 4.3, a simple method can be devised to measure the target distance s_0 through the self-mixing effect. Typical values for the parameters appearing in (10) are $\lambda_0 = 850$ nm, $s_0 = 1$ m, $\chi = 10$ pm mA^{-1} and $Y = 20$ mA V^{-1} [22], and the corresponding value for the responsivity is $\Re = 4.25$ mV μm^{-1}.

A comment on the nature of the responsivity of the self-mixing vibrometer is worthwhile. In this approach, *displacement* is the variable that is converted into an electrical signal. This will be compared with conventional LDVs, where *velocity* is the measured variable. This fact implies relevant differences in the noise equivalent vibration and the dynamic range of the two types of instrument.

So far, for the sake of simplicity, we have neglected the dependence of the power emitted by the LD on injected current. This is represented by the 'P/I characteristic' block in figure 4, i.e. a power variation $\Delta P_I = \eta \Delta I$ is generated, where η is the LD slope efficiency. To make the above exposed operating principle work properly, the power modulation effect must be cancelled. This is performed by the compensation loop (blocks enclosed in the dashed box in figure 4), that simply subtracts the unwanted signal term caused by power modulation. The compensation path must be trimmed so as to match the effective slope efficiency of the used LD. Finally, a proper DC offset is applied to compensate for the CW power level emitted by the unperturbed LD.

4.1. Noise

The minimum measurable vibration amplitude is limited by noise. Three noise sources can be identified:

 (i) shot noise associated with the photodetected current;
 (ii) interferometer phase noise caused by the finite LD linewidth [23];
(iii) mechanical noise of the optical set-up from environment disturbance, which generally has a $1/f$ spectrum.

Phase noise is converted into amplitude noise through the slope β of the transfer characteristic of the self-mixing interferometer (see figure 3). Calculations show that, for LD linewidth below 10 MHz, shot noise dominates over phase noise for target distances $s_0 < 10$ m.

The S/N ratio attained by the servo-vibrometer is basically the same as that of the conventional open-loop self-mixing interferometer. The shot-noise current is given by

$$I_n^2 = 2q\sigma F P_0 B \qquad (11)$$

where q is electron charge, σ is net photodiode responsivity, F is the excess-noise factor (typically $F = 2$), P_0 is the power emitted by the LD and B is the measurement bandwidth. In the moderate feedback regime ($C > 1$) the slope β of the transfer characteristic of the self-mixing interferometer is given by [7, 24]

$$\beta = \gamma \frac{P_0}{s_0} \;\; (\text{W rad}^{-1}) \qquad (12)$$

where the factor γ (m rad^{-1}) depends on the photon lifetime and the enhancement linewidth factor of the LD [7, 24]; a typical value is $\gamma = 1.45 \times 10^{-4}$ m rad^{-1}. The photocurrent signal corresponding to a displacement Δs is thus given by

$$I_s = \sigma \beta \Delta s \frac{2\pi}{\lambda/2} = \sigma \gamma \frac{2\pi}{\lambda/2} \frac{P_0}{s_0} \Delta s. \qquad (13)$$

The S/N ratio is calculated as $S/N = I_s^2/I_n^2$. By letting $S/N = 1$, we find the vibrometer noise equivalent vibration as

$$\Delta s_{min} = \frac{\lambda}{2\gamma\pi} \sqrt{\frac{qFB}{2\sigma P_0}} s_0. \qquad (14)$$

Apart from the obvious dependence on LD power, it can be noticed that the noise equivalent vibration worsens for increasing target distance, because of the decrease of the slope transfer characteristic β with s_0, as shown by (12). The latter is an intrinsic characteristic of self-mixing interferometry in the moderate feedback regime (e.g., for values of the feedback parameter $C \geqslant 1$), in which the modulation index m does not further increase for increasing optical feedback. For an emitted power $P_0 = 10$ mW, net monitor photodiode responsivity $\sigma = 0.02$ A W^{-1}, and target distances s_0 of 0.1 and 1 m, equation (14) yields sensitivities of 2.5 pm Hz$^{-1/2}$ and 25 pm Hz$^{-1/2}$ respectively. These figures are indeed remarkable, and they can be attained in practice even on rough surfaces using a simple optical arrangement. The noise equivalent vibration of the self-mixing vibrometer is, in principle, constant over frequency, and a white noise floor is obtained for the displacement vibration variable.

4.2. Maximum measurable vibration

The amplitude of the maximum measurable vibration is limited by the finite value of the open-loop gain, and by inaccuracy in the calibration of the compensation loop (see figure 4). As a consequence, in practice the value of the interferometer phase is not kept at a constant value, i.e. a phase error $\Delta\phi_{err}$ exists, which is proportional to target vibration amplitude. When $\Delta\phi_{err} = \pi$, a fringe jump occurs, and the output signal is no longer proportional to the vibration, causing distortion. For $G_{loop} = 500$, the effects on the phase error caused by finite open-loop gain and residual inaccuracy in the compensation loop are comparable, and the maximum measurable vibration is

$$\Delta s_{max,1} \approx G_{loop}(\lambda_0/4) = 100 \; \mu\text{m}. \qquad (15)$$

From figures 2(d) and (e), it is noticed that for increasing optical backreflection the signal hysteresis increases, thus increasing also the useful width of the interferometric fringe beyond the conventional 2π value. This effect results in an extension of the dynamic range as calculated by equation (15).

Another limitation to the maximum measurable vibration may arise due to the limited continuous tunability range of LD wavelength, which is typically $\Delta\lambda_{max} = 200$ pm for an F–P LD. From equation (4), we obtain

$$\Delta s_{max,2} = (\Delta\lambda_{max}/2\lambda_0)s_0 \qquad (16)$$

hence this limitation is less severe for large target distances. For $s_0 = 1$ m we have $\Delta s_{max,2} = 125 \; \mu$m. Obviously, the attainable dynamics will be determined by the minimum between $\Delta s_{max,1}$ and $\Delta s_{max,2}$.
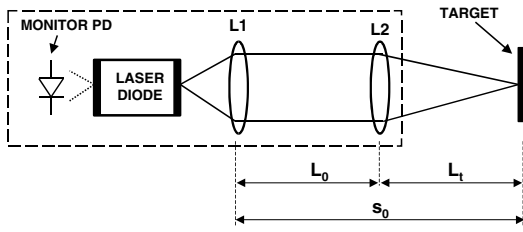
Figure 5. Experimental optical arrangement for the self-mixing vibrometer. L1, objective lens; L2, focusing lens. $L_0 = L_t = 0.4$ m.

4.3. Precision and accuracy

The instrument's precision and accuracy depend on how accurate is the knowledge of the parameters appearing in the responsivity expression of equation (10). First of all, the dependence of the responsivity on the target distance s_0 is not of concern. In fact, the self-mixing interferometric configuration itself allows us to easily measure the target distance through LD wavelength sweeping [16, 17], and the vibrometer instrument can thus be used also for target ranging in those applications requiring this feature. The principle of distance measurement relies on the generation of a self-mixing interferometric signal by means of an LD wavelength sweep of known amplitude, obtained by applying a triangular modulation to the LD current. By counting the number of interefrometric fringes generated within one period, the distance can be retrieved, with an accuracy as good as 10^{-3} for distances s_0 around 1 m [17]. So, periodically or at the beginning of a measuring session, the procedure of distance measurement shall be carried out, and the responsivity calibrated accordingly through adjustment of a multiplicative factor on the output signal, which can be performed automatically.

The coefficient χ of wavelength drift versus injected current has a very small dependence on LD temperature and ageing. Larger variations are expected on the absolute value of the emitted wavelength λ_0. For an F–P LD with no active temperature control, a variation of $10\,°C$ in the operating temperature can be expected, resulting in a precision on the wavelength of 5×10^{-3}. By controlling the LD temperature within $0.1\,°C$, a residual uncertainty remains due to the possibility of longitudinal mode jumps, and a typical value for the precision is 5×10^{-4}. In conclusion, the overall precision can attain 10^{-3} (i.e. 0.1% of actual output signal reading) with LD temperature control, while the short-term accuracy can be better than 10^{-3} even without temperature control.

5. Experimental results

The typical optical experimental arrangement for the self-mixing laser vibrometer is shown in figure 5. A commercial single-longitudinal-mode Fabry–Perot LD emitting 40 mW maximum power at 800 nm is used. One objective lens collimates LD radiation, and a second focusing lens placed at a distance $L_0 = 40$ cm projects the laser spot on the diffusing target under measurement. The target is placed at a distance $L_t = 40$ cm from the output lens (corresponding to its focal length), hence the LD-to-target distance is $s_0 = 80$ cm. This optical set-up ensures an efficient coupling of the backscattered
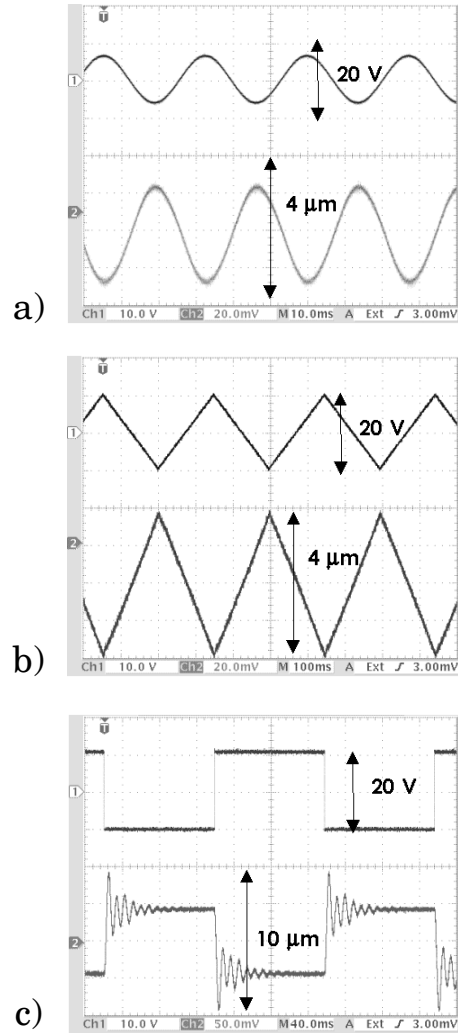

Figure 6. Examples of vibration measurement for different drive signals. The target is a loudspeaker with a black paper surface. Upper traces, loudspeaker drive signal; lower traces, vibrometer output signal, with 20 mV μm^{-1} responsivity. (a) 30 Hz sine vibration; (b) 3 Hz triangular wave; (c) 10 Hz square wave; damped resonance oscillations of the loudspeaker are clearly visible.

light into the LD cavity, so that the moderate feedback regime ($C > 1$) is easily attained on most rough surfaces. The electronic feedback loop is built using conventional high speed operational amplifiers, and a loop gain of 500 is obtained.

The system has been tested using a loudspeaker with a black paper cone as target. Figure 6 reports the experimental output vibration waveforms detected when the loudspeaker is driven by a sine, a triangle and a square signal at different frequencies. The output signal from the vibrometer is a perfect analogue replica of the target displacement. Correctness of the measured vibration waveforms has been assessed by comparison with a conventional He–Ne laser interferometer. It should be noted that measured vibration amplitudes shown in figure 6 are much larger than the width of the interferometric fringe, $\lambda/2$.

The vibrometer responsivity has been measured for different LD-to-target distances, by varying the distance L_0 between the two lenses. The results reported in figure 7 confirm the prediction of formula (10) for values of s_0 up to 6 m.
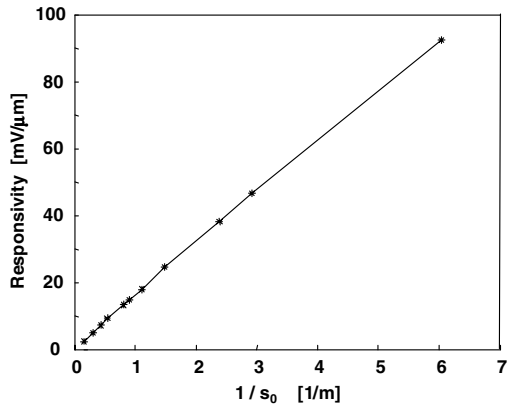
Figure 7. Measured responsivity of vibrometer output signal (mV μm^{-1}) as a function of the reciprocal of LD-to-target distance s_0.
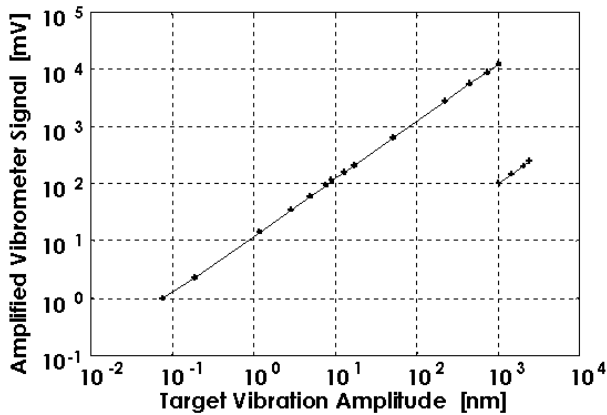

Figure 8. Vibrometer linearity: measured vibrometer output signal as a function of target vibration amplitude. Target distance is 16.5 cm; vibration frequency is 924 Hz; noise floor is 2 mV within 1 Hz bandwidth. The measurement is carried out using an FFT analyser. The vibrometer signal is amplified 20 dB for vibrations smaller than 1 μm.

Bandwidth measurements have revealed that the responsivity is constant up to the 70 kHz cut-off frequency, which corresponds to the calculated value of the closed-loop gain. The latter is determined by the value of the DC open-loop gain and by the frequency of the compensating pole.

Vibrometer linearity can be assessed by looking at figure 8, that reports the measured output as a function of vibration amplitude in a logarithmic scale. A dynamic range larger than 100 dB is achieved, and the linearity is better than 0.1% of full scale.

Figure 9 reports the measured and calculated values for both the noise equivalent vibration and the maximum measurable vibration amplitude as a function of frequency for a target distance $s_0 = 0.8$ m. The measured noise floor is as low as 20 pm Hz$^{-1/2}$ at 1 kHz, and it increases at lower frequencies due to $1/f$ microphonics from the ambient. At higher frequencies the noise equivalent vibration worsens due to the decrease in the responsivity.

The maximum measurable vibration basically depends on the frequency response of the open-loop gain, as given by equation (15). The maximum measurable vibration amplitude is 180 μm (peak to peak), in a frequency range between 0.1 and 100 Hz.
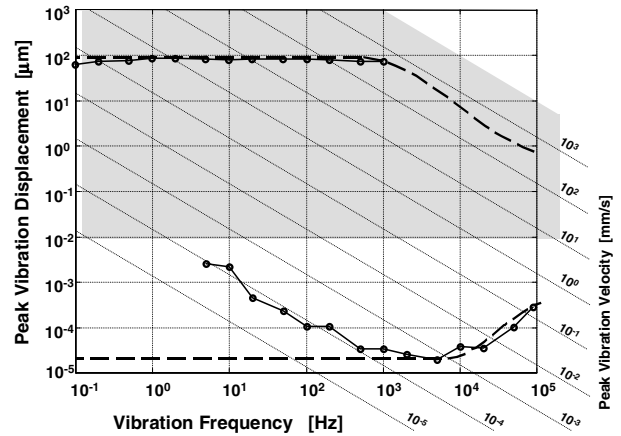

Figure 9. Normogram plane reporting the performance of the self-mixing vibrometer in terms of maximum measurable vibration amplitude and noise equivalent vibration limit (measured within 1 Hz bandwidth in laboratory conditions). Thick dashed curve: calculated values. Thin solid curve and circles: measured values. LD-to-target distance is $s_0 = 0.8$ m; the target is a loudspeaker with a black paper cone. Maximum vibration amplitude beyond 1 kHz could not be measured due to limitations of vibrating apparatus. For comparison purposes, the shaded area summarizes the operating range of a high resolution commercial LDV [27].

Figure 10. Photograph of prototype self-mixing LD vibrometer. Left, electronic unit; right, optical head.

From equations (14) and (16) it is clear that there exists an optimum target distance s_0, resulting from the trade-off between noise equivalent vibration and maximum measurable vibration. However, the vibrometer guarantees more than 100 dB dynamic range irrespective of the choice of s_0.

6. Instrument development

Given the good results obtained from the self-mixing laser vibrometer, a prototype instrument has been designed and built. Figure 10 shows a photograph of the instrument, which is made of an optical head and an electronic unit. The optical head contains the LD, the trans-impedance amplifier, the collimating objective and the focusing lens. A good compromise between noise equivalent vibration and maximum vibration amplitude is obtained by choosing $s_0 = 0.8$ m. The instrument working distance (i.e. the distance between the optical head and the surface under test) is chosen as $L_t = 0.4$ m, and the distance between the two lenses is $L_0 = 0.4$ m (see figure 5). The optical path between the two lenses is folded to reduce the optical head dimensions. The electronic unit contains the power supplies, one printed circuit board implementing the feedback loop, one dedicated to LD current modulation and
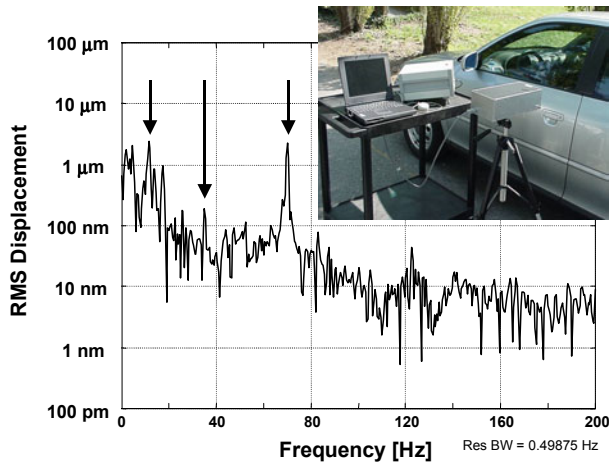
Figure 11. Example of instrument use in the field. The optical head is aimed at the body of a car with its four-stroke engine running at 2100 rpm (see inset). The graph shows the vibration spectrum as obtained by FFT of a single-shot acquisition. The fundamental frequency at 35 Hz is clearly seen, together with the large second harmonic at 70 Hz (sparkle events) and suspension resonance frequency (at 13 Hz), all indicated by arrows. In this measurement, mechanical environmental disturbances generate a noise floor larger than that shown in figure 9.

one board for the elaboration of the output signal, in order to display the vibration frequency and its RMS amplitude on the seven-segment indicators on the front panel. The output signal is provided at a BNC output, with a responsivity of 10 mV μm^{-1}.

When the object under test has a rough diffusing surface, the backscattered light is affected by the speckle-pattern statistics [25], and it may happen that the power fed back into the LD cavity is too small, thus causing signal fading. However, by slightly changing the position of the laser spot projected on the target, it is always possible to find a 'bright' speckle. So, a 'search' procedure is performed before starting the measurement session. For this purpose, the focusing lens is mounted on a slide actuated by a screw that allows us to transversally move the laser spot position on the target surface, while a meter on the front panel helps in maximizing the intensity of the optical feedback. This procedure could also be performed automatically. Obviously, the instrument can also work on co-operative targets, and in this case an optical attenuator will be inserted in the optical path to prevent optical feedback from becoming excessive. When a diffusive target exhibits an in-plane vibration component transversal to the laser beam, signal drop-outs may occur, due to changes in the speckle distribution. For the self-mixing vibrometer, that operates with a focused beam on the target, a transversal displacement of about 80 μm can be tolerated, as this is the target displacement that, on average, causes signal fading on a white paper target [5]. This figure also corresponds to the transversal position resolution attainable by the instrument.

The instrument performed satisfactorily in a variety of test measurements carried out both in laboratory environment and in the field. As an example, figure 11 reports the vibration spectrum obtained when aiming the self-mixing laser vibrometer at the body of a car with its four-stroke engine running at 2100 rpm. The fundamental frequency at 35 Hz is clearly

seen, together with the large second harmonic at 70 Hz (sparkle events), suspension resonance frequency (at 13 Hz) and $1/f$ mechanical noise. The prototype was also successfully tested to measure the small movement (in the sub-μm range) of a micro-electro-mechanical system (MEMS) device [26].

The measured noise equivalent vibration and dynamic range of the instrument are consistent with those reported in figure 9. The performance of the self-mixing vibrometer and of a high quality high resolution commercial LDV [27] are also compared in the normogram plane of figure 9. The prototype self-mixing vibrometer has a better noise equivalent displacement, and it is limited in the high frequency high velocity region of the plane, where the performance of the LDV is better, by more than an order of magnitude. However, the dynamic range of the self-mixing vibrometer can be further expanded towards large vibrations by using a technique now under development. We foresee that vibration amplitudes of 1 mm peak to peak are in the reach of the instrument, as well as the 1 m s^{-1} velocity limit.

As far as the emission wavelength is concerned, either for safety or visibility considerations, two remedies can be proposed:

(i) use of a visible pointing beam generated by a red LD superimposed on the measuring beam;
(ii) direct use of a visible LD as the source for the self-mixing vibrometer, because the operating principle has been already demonstrated with several LD specimens.

Finally, the depth of field of the instrument, i.e. the longitudinal displacement of the target around the optimal working distance that causes a factor of two reduction in the dynamic range, is $\pm$8 cm.

7. Conclusions

A new type of laser vibrometer based on the self-mixing interferometric effect in an LD has been demonstrated. The proposed method has been investigated both theoretically and experimentally, achieving a good agreement between design specifications and attained performance. A prototypal instrument has been designed, built and tested, obtaining the following figures: better than 100 pm Hz$^{-1/2}$ noise equivalent vibration, 180 μm peak-to-peak maximum measurable vibration, larger than 100 dB dynamic range, 70 kHz bandwidth, successful operation on most rough surfaces.

The self-mixing laser vibrometer can find application in most cases where non-contact operation is required (i.e. for monitoring of soft or lightweight structures) and it is also advisable for modal testing, where the vibration of a large surface can be monitored by scanning the laser beam position. Other applications involve composite material analysis and testing, noise and vibration measurements in industrial and scientific environments, loudspeaker and PZT characterization and PZT accelerometer calibration. Use of the instrument is also advisable to replace non-optical vibration sensing methods, because the small noise equivalent vibration allows us to relax power requirements of the shaker/stimulus apparatus.

The proposed approach is intrinsically low cost, since it relies on a minimum part-count uncomplicated optical set-up and on straightforward signal processing, owing to the simplicity and effectiveness of the self-mixing interferometric configuration.

References

[1] Drain L E 1980 *The Laser Doppler Technique* (New York: Wiley)
[2] Tomasini E P, Revel G M and Castellini P 2001 Laser based measurements *Encyclopaedia of Vibration* (London: Academic) pp 699–710
[3] Castellini P, Revel G M and Tomasini E P 1998 Laser Doppler vibrometry: a review of advances and applications *Shock Vib. Dig.* **30** 443–56
[4] Pickering C J D and Halliwell N A 1986 The laser vibrometer: a portable instrument *J. Sound Vib.* **107** 471–85
[5] Giuliani G, Donati S and Monti L 2002 Self-mixing laser diode vibrometer with wide dynamic range *5th Int. Conf. on Vibration Measurements by Laser Techniques: Advances and Applications (SPIE Proc. vol 4827)* ed E P Tomasini (Bellingham, WA: SPIE) pp 353–62
[6] Bosch T, Servagent N and Donati S 2001 Optical feedback interferometry for sensing applications *Opt. Eng.* **40** 20–7
Donati S and Merlo S 1998 Applications of diode laser feedback interferometry *J. Opt.* **29** 156–61
[7] Giuliani G, Norgia M, Donati S and Bosch T 2002 Laser diode self-mixing technique for sensing applications *J. Opt. A: Pure Appl. Opt.* **4** S283–94
[8] Donati S, Giuliani G and Merlo S 1995 Laser diode feedback interferometer for measurement of displacements without ambiguity *IEEE J. Quantum Electron.* **31** 113–19
[9] Rudd M J 1968 A laser Doppler velocimeter employing the laser as a mixer–oscillator *J. Phys. E: Sci. Instrum.* **1** 723–6
[10] Wang W M, Grattan K T V, Palmer A W and Boyle W J O 1994 Self-mixing interference inside a single-mode diode laser for optical sensing applications *J. Lightwave Technol.* **12** 1577–87
[11] Paone N and Scalise L 2002 Vibrometry based on self-mixing effect *Opt. Lasers Eng.* **38** 173–84
[12] Acket G A, Lenstra D, Den Boef A J and Verbeek B H 1984 The influence of feedback intensity on longitudinal mode properties and optical noise in index-guided semiconductor lasers *IEEE J. Quantum Electron.* **20** 1163–9
[13] Donati S 1978 Laser interferometry by induced modulation of the cavity field *J. Appl. Phys.* **49** 495–7
[14] Servagent N, Gouaux F and Bosch T 1998 Measurements of displacement using the self-mixing interference in a laser diode *J. Opt.* **29** 168–73
[15] Beheim G and Fritsch K 1986 Range finding using frequency modulated laser diode *Appl. Opt.* **25** 1439–42
[16] Shinohara S, Yoshida H, Ikeda H, Nishide K and Sumi M 1992 Compact and high-precision range finder with wide dynamic range and its application *IEEE Trans. Instrum. Meas.* **41** 40–4
[17] Gouaux F, Servagent N and Bosch T 1998 Absolute distance measurement with an optical feedback interferometer *Appl. Opt.* **37** 6684–9
[18] Shinoara S, Mochizuki A, Yoshida H and Sumi M 1986 Laser Doppler velocimeter using the self-mixing effect of a semiconductor laser diode *Appl. Opt.* **25** 1417–19
[19] Scalise L, Steenbergen W and De Mul F F 2001 Self-mixing feedback in a laser diode for intra-arterial optical blood velocimetry *Appl. Opt.* **40** 4608–15
[20] Koelink K, de Mul F F M, Weijers A L, Greve J, Graaff R, Dassel A C M and Aarnoudse J G 1994 Fiber-coupled self-mixing diode laser Doppler velocimetry: technical aspects and flow velocity profile disturbance in water and blood flow *Appl. Opt.* **33** 5628–41
[21] Ozdemir S K, Shinohara S, Ito S and Yoshida H 2001 Compact optical instrument for surface classification using self-mixing interference in a laser diode *Opt. Eng.* **40** 38–43
[22] LDC 202 laser controller datasheet, Profile GmbH
[23] Giuliani G and Norgia M 2000 Laser diode linewidth measurement by means of self-mixing interferometry *IEEE Photon. Technol. Lett.* **12** 1028–30
[24] Giuliani G and Donati S 1999 Analysis of the signal amplitude regimes in injection-detection *Proc. IEEE-LEOS ODIMAP II, 2nd Topical Meeting on Optoelectronic Distance/Displacement Measurements and Applications (Pavia, 1999)* pp 75–80
[25] Dainty J C (ed) 1984 *Laser Speckle and Related Phenomena* (Berlin: Springer)
[26] Annovazzi-Lodi V, Merlo S and Norgia M 2001 Measurement on a micromachined silicon gyroscope by feedback interferometry *IEEE/ASME Trans. Mechatron.* **6** 1–6
[27] OVD-20 demodulator for OFV-3001 vibrometer controller datasheet, Polytec GmbH, http://www.polytec.com